A mechanistic investigation of the Pd-catalyzed cross-coupling between *N*-tosylhydrazones and aryl halides

Gilian T. Thomas*, Kiera Ronda, J. Scott McIndoe*

Department of Chemistry, University of Victoria, PO Box 1700 STN CSC, Victoria, BC V8W 2Y2, Canada.
Fax: +1 (250) 721-7147; Tel: +1 (250) 721-7181; E-mail: gilian.t.thomas@gmail.com, mcindoe@uvic.ca

Abstract

The cross-coupling of *N*-tosylhydrazones and aryl halides forms carbon-carbon bonds, producing 1,1-disubstituted alkenes. Though it has proven extremely useful in several fields of chemistry, its mechanism remains experimentally unexplored. Combining benchtop NMR and real-time mass spectrometry afforded the ability to monitor the catalytic intermediates as well as the rate of product formation.

Graphical abstract

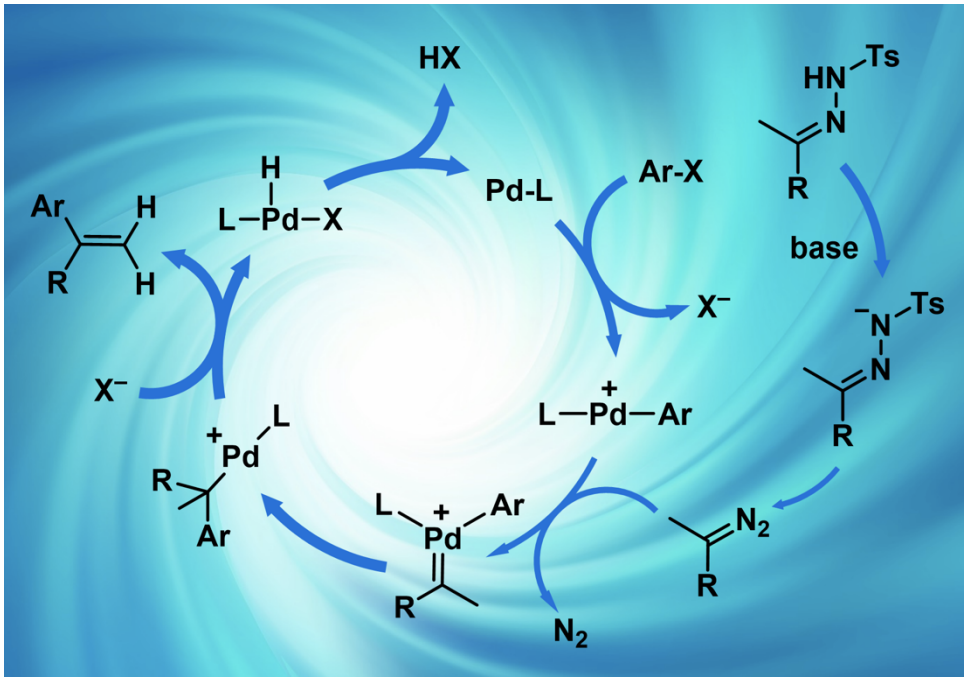

The formation of carbon-carbon bonds is essential to many fields including, but not limited to, pharmaceutical synthesis,[1] medicinal chemistry,[2,3] natural products,[4–7] and materials.[8] Palladium catalysis is one of the most common and reliable methods of carbon-carbon bond formation, especially for late-stage assembly of two segments in a total synthesis,[9–17] and this area was recognized with the awarding of the 2010 Nobel Prize in Chemistry to Suzuki, Heck, and Negishi.[18]

The Barluenga cross-coupling reaction has emerged more recently as an efficient method of accessing carbon-carbon bonds.[19] A palladium catalyst is used to form a carbon-carbon bond between an *N*-tosylhydrazone and an aryl halide, mainly alkyl bromides.[19] The substrate scope has since been extended to provide access to a variety of products, including but not limited to benzyl halides,[20] aryl nonaflates,[21] and alkenyl halides.[22] *N*-tosylhydrazones as cross-coupling partners alleviate the need for stoichiometric amounts of organometallic reagents, and can easily be produced from the corresponding ketone or aldehyde *in situ*.[23,24] In contrast to the Mizoroki-Heck cross-coupling reaction, the Barluenga cross-coupling does not require an alkene as a coupling partner, and produces a geminal alkene rather than a *trans*-alkene. Due to its advantageous functional group tolerance, this cross-coupling reaction has vast potential in synthetic chemistry, and proven applications in cancer treatments,[25] natural product synthesis,[26,27] and polymer synthesis.[28]

Based on the fact that *N*-tosylhydrazones exhibit nucleophilic behaviour, in combination with previous palladium studies, Barluenga and coworkers[19] proposed the mechanism to begin with oxidative addition of the organic halide to the active palladium(0) complex (Figure 1). The *N*-tosylhydrazone undergoes base-mediated decomposition, and the product then binds to the palladium complex, resulting in a palladium-carbene complex. It is suggested that this complex would then undergo migratory insertion of the aryl group to produce an alkyl palladium complex. In the final step, β-hydrogen elimination generates the aryl olefin product, and regenerates the initial palladium(0) active catalyst species. The catalytic mechanism has been studied computationally,[29,30] however reaction intermediates for this catalytic cycle have yet to be observed experimentally.

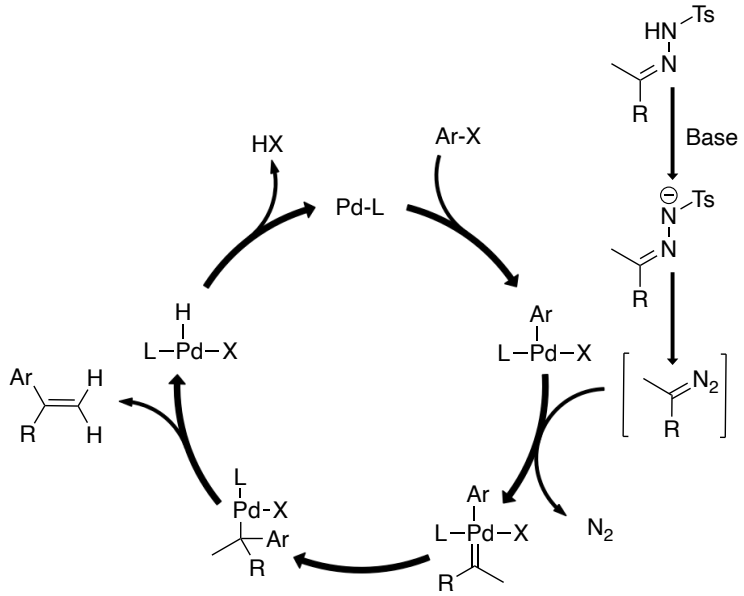

Figure 1. Proposed catalytic cycle of the reaction between *N*-tosylhydrazones and aryl halides.[19]

Herein, we report examination of the mechanism of the cross-coupling between *N*-tosylhydrazones and aryl bromides. Catalytic intermediates are studied in real-time by pressurized sample infusion-electrospray ionization-mass spectrometry (PSI-ESI-MS), and the overall reaction progress is monitored by benchtop NMR spectroscopy.

In order to adapt the heterogeneous reaction conditions developed by Barluenga, a reaction screen was carried out in search of homogeneous conditions to facilitate accurate offline sampling, as well as online monitoring via PSI-ESI-MS.[31,32] Several bases, solvents and catalysts were analyzed in combination with the SPhos ligand, but only a few generated product, and only one generated product and was homogeneous (see supplementary information). The lack of product generated while screening dioxane as a solvent was contradictory to the results of Barluenga,[19] however this is attributed to the use of stock solutions in this reaction screen as not all reagents were soluble in dioxane. A control reaction in dioxane with heterogeneous reaction components was successful outside of the reaction screen. Homogeneous reaction conditions were found in methanol, catalyzed by $Pd(OAc)_2$ with sodium *tert*-butoxide as a base. Further analysis led to a ternary solvent system composed of methanol, toluene, and tetrahydrofuran (1:1:1), as toluene allowed the reaction to be run at higher temperatures and THF improved the solubility of reagents. After the solvent system was finalized, the reaction was performed with the precatalyst $Pd_2(dba)_3$ and was found to increase the rate of the reaction compared to $Pd(OAc)_2$ under these conditions, and was carried forward for reaction monitoring.

The reaction was monitored using a Nanalysis 60 MHz NMR instrument.[33] Reaction monitoring was carried out over 48 hours to determine the rate of product formation under homogeneous conditions (see supplementary information). The reaction was observed to be complete after 24 hours as the concentration of product did not increase from 24 to 48 hours. Results from a 300 MHz NMR spectrometer mapped closely to that of the benchtop instrument (see supporting information). All reactions were quantified using the distinct alkene signal at 5.43 ppm as it occupies a region of the spectrum free from any other signals.

Benchtop NMR spectrometers do not require liquid helium nor liquid nitrogen to maintain the temperature of the magnet, and the permanent magnets used can be influenced by the temperature in the room.[34] To ensure reproducibility, the reaction was performed in triplicate using the now-established homogeneous reaction conditions (Figure 2, inset).

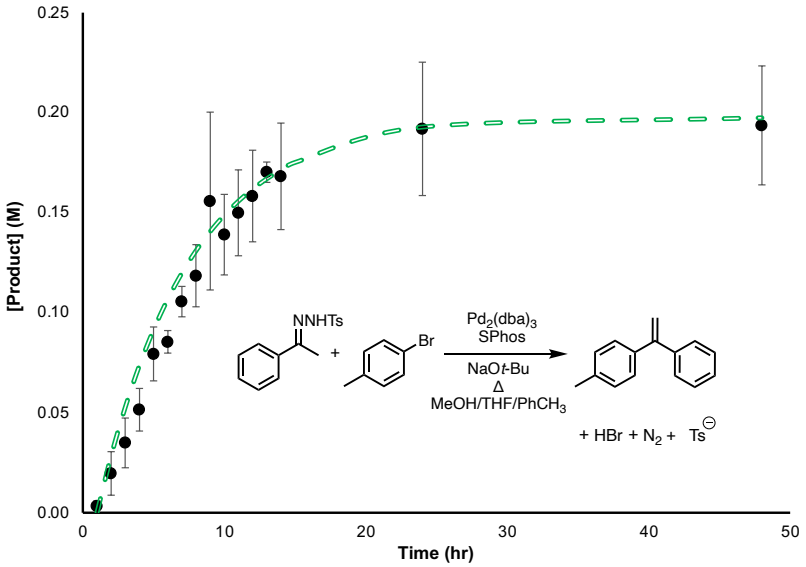

Figure 2. ^{1}H-NMR reaction monitoring using final reaction conditions based on screen (inset) over 48 hours, error bars indicate triplicate experiments. Dashed green line represents a first order fit with a 1 hour induction period. Conditions: 1% [Pd], 2% SPhos, 0.003 mol acetophenone tosylhydrazone, 0.003 mol bromotoluene, 0.0067 mol NaO*t*-Bu, 70ºC.

The rate of reaction is approximately constant for hours 1-10, following an induction period of approximately one hour. The overall reaction kinetics appear to be first order. Further interrogation of the rate of reaction (see supporting information) showed the reaction was not accelerated by doubling the bromobenzene concentration, but it approximately doubled upon addition of two equivalents of the tosylhydrazone. Upon introducing *para*-substituents on the aryl bromide substrate, maximum rates were subjected to a Hammett analysis (Figure 3). Five substituents with varying electron-withdrawing and electron-donating capabilities were compared to the H reference substituent, however no clear differences in rate were observed, with all rates being well within the same order of magnitude. This insensitivity contrasts with data from a related oxidative addition reaction (trendline for which are shown on Figure 3), many of which display the same sort of reactivity pattern as is observed for the oxidative addition step alone. Others have also found similar insensitivity of substitution patterns for bromoanilines in this reaction.[35]

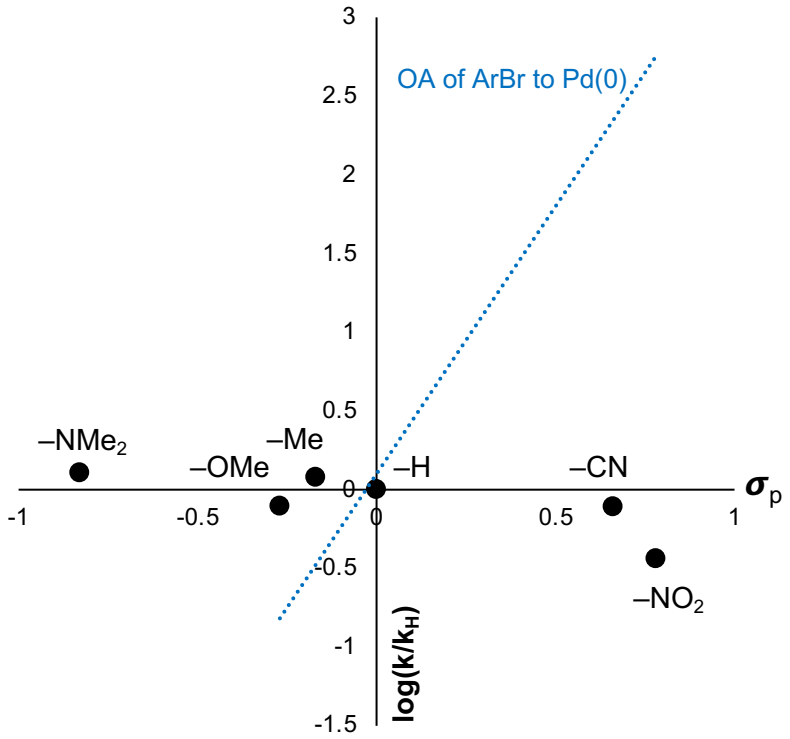

Figure 3. Hammett plot of $\log(k/k_H)$ vs. Hammett parameter (σ_p)[36] for *para*-substituted aryl bromides as labelled. k represents the initial reaction rate of each substituent, and k_H represents the initial reaction rate of the H-substituted substrate. The trendline represents the oxidative addition of *para*-substituted aryl bromides to Pd(0) as reported by Lu et al.[37]

Given the insensitivity to substituent effects, we compared the bromobenzene data to that of iodobenzene and chlorobenzene (Figure 4). The chlorobenzene reaction did prove to be much slower, with no product detected before the 3 hour mark in the reaction and a rate of 0.001 mol L^{-1} s^{-1}. Iodobenzene got off to a faster start but the reaction rate after the first hour (0.017 mol L^{-1} s^{-1}) was essentially identical to that of the bromobenzene (0.015 mol L^{-1} s^{-1}). This result suggested that oxidative addition is not controlling the overall rate of reaction except in the case of the chlorobenzene. The higher initial rate for iodobenzene suggests that the oxidative addition reaction is fast enough that it does not limit the rate even at the start of the reaction. We concluded that the turnover limiting step lies off-cycle for aryl iodides and bromides, this being the transformation of the *N*-tosylhydrazone into the active dinitrogen intermediate. For the chlorobenzene, oxidative addition is most likely the turnover-limiting step.

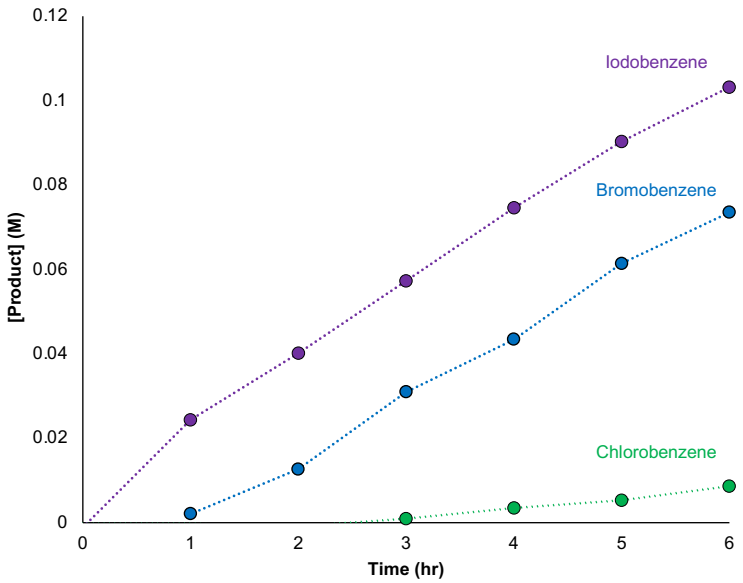

Figure 4. Effect of aryl halide on the initial rate of product formation. Conditions: 1% [Pd], 2% SPhos, 0.003 mol acetophenone tosylhydrazone, 0.003 mol ArX, 0.0067 mol NaO*t*-Bu, 70ºC.

For further insights into the reaction, we probed the system using electrospray ionization mass spectrometry. ESI-MS analysis requires charged species to accurately observe catalytic intermediates.[38] In this case, a sulfonated SPhos (sSPhos) ligand was an ideal candidate as it is very similar to SPhos, which was used throughout this study up to this point, and has an inherent negative charge. In a control reaction, sSPhos was found to have the same kinetic profile as SPhos (see supporting information), indicating that the presence of a sulfonate group does not significantly change the reaction.

Initial PSI-ESI-MS analysis (Figure 5) involved a solution of sSPhos (L, the charge-tagged ligand) to which sequential addition of $Pd_2(dba)_3$, bromotoluene and a mixture of acetophenone tosylhydrazone and sodium *tert*-butoxide were added. Coordination of L to palladium occurred rapidly, with the production of $[LPd(dba)]^-$ proceeding to completion with a half-life of approximately 0.9 minutes. Oxidative addition of bromotoluene to $[LPd(dba)]^-$ to form $[LPd(Tol)Br]^-$ was slower, with the disappearance of the $[LPd(dba)]^-$ following pseudo first order kinetics with a half-life of 7.6 minutes.

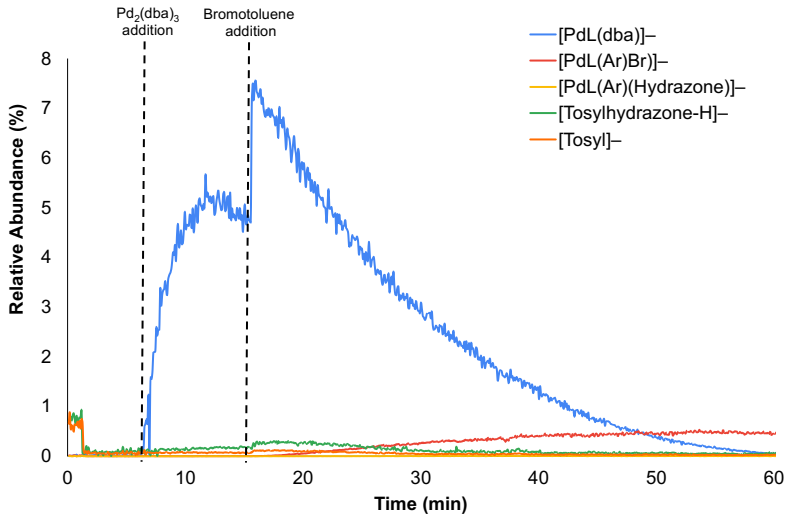

Figure 5. PSI-ESI-MS monitoring of the oxidative addition of bromotoluene to Pd(sSPhos)(dba).

However, the appearance of product $[Pd(L)(Ar)(Br)]^-$ did not remotely match the amount of reactant being consumed, suggesting that the difference in peak heights was something other than a discrepancy in ion response factor. As there were no other anions appearing during this process, it seemed likely that the "missing" ion intensity was the result of charge neutralization via formation of a zwitterion (not visible in either ion mode). To test this assumption, we looked at the same reaction but with neutral SPhos, so that any species with a positive charge would instead be cationic rather than zwitterionic, and detectable in the positive ion mode.

$[Pd(SPhos)(Ar)]^+$ was observed to form after the addition of bromotoluene in positive ion mode, suggesting that the zwitterion was indeed Pd(L)Ar (i.e. the positive charge of the complex is cancelled out by the negative charge on the ligand). To confirm that the missing $[Pd(L)(Ar)(Br)]^-$ is sequestered as Pd(L)(Ar), the mass spectrometer was operated in positive ion mode and negative ion mode simultaneously, monitoring both reactions under identical conditions (Figure 6). $Pd_2(dba)_3$ was combined with both SPhos and sSPhos in a flask and allowed to stir at 70°C. The catalyst activation step was deemed complete upon the establishment of a stable signal of $[Pd(L)(dba)]^-$. Bromotoluene was added to the reaction vessel to initiate the oxidative addition step. In negative ion mode, $[Pd(sSPhos)(dba)]^-$ (Figure 6, red trace) began decreasing in intensity as expected, and hardly any $[Pd(L)(Ar)(Br)]^-$ formed, as previously observed (Figure 6, blue trace). In positive ion mode, an immediate increase in $[Pd(L)(Ar)]^+$ was observed (Figure 6, green trace), demonstrating a dissociative equilibrium between [Pd(L)(Ar)(Br)] and Pd(L)(Ar) that lies towards Pd(L)(Ar).

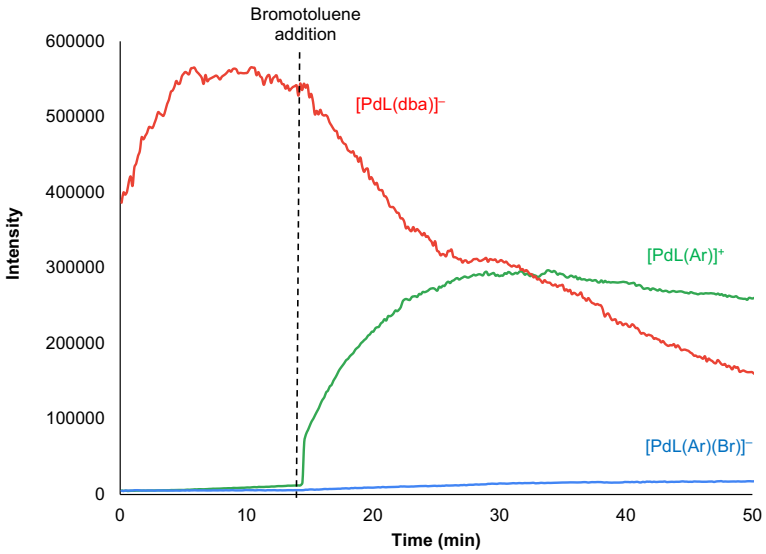

Figure 6. Negative ion mode monitoring of $[Pd(sSPhos)(dba)]^-$ and $[Pd(sSPhos)(Ar)(Br)]^-$ overlaid with rescaled positive ion mode monitoring of $[Pd(SPhos)(Ar)]^+$.

Upon addition of acetophenone tosylhydrazone and sodium *tert*-butoxide the spectrum became completely dominated by deprotonated acetophenone tosylhydrazone and the tosyl anion, indicating that the excess charged base effectively suppressed ions from any other source, and the spectrum became bereft of any palladium-containing ions (Figure 7).

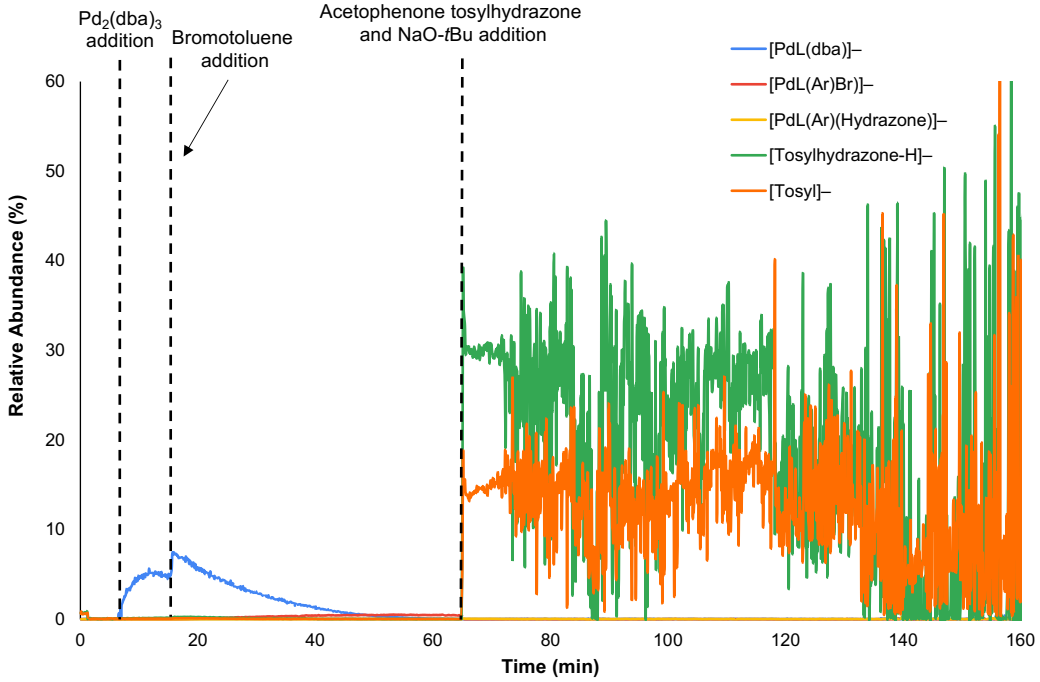

Figure 7. Complete PSI-ESI-MS monitoring trace of the Pd-catalyzed reaction between acetophenone tosylhydrazone and bromotoluene.

The combination of PSI-ESI-MS and NMR provides complementary information on the mechanism. The ESI-MS results show that the catalyst activation and oxidative addition steps are both fast enough to not affect reaction turnover, but the oxidative addition step is slow enough for aryl bromides that it can account for an induction period not observed for aryl iodides. PSI-ESI-MS also shows that after oxidative addition, the reaction is partitioned primarily as the cationic $[(\text{phosphine})\text{Pd}(\text{Ar})]^+$, although this species is in equilibrium with the neutral (phosphine)Pd(Ar)(X). Addition of tosylhydrazone and base showed that the deprotonation and tosyl dissociation steps are both very fast. We do not see any further palladium-containing intermediates due to ion suppression effects from the added base, but NMR evidence provides pointers as to why we may well not have seen anything even if this effect was not operational. Doubling the bromotoluene concentration had no effect on rate, nor did changing substituents on the aryl ring, but doubling the tosylhydrazone concentration doubled the rate of reaction. Putting all this information together, the evidence points towards a reaction whose palladium-containing resting state is the cationic oxidative addition product in all cases except for chlorobenzenes, and whose overall rate is controlled by its reaction with the diazo derivative derived from the tosylhydrazone decomposition. As such, efforts to improve the reaction should seriously consider focusing on the acceleration of this step.

References

1 K. R. Campos, P. J. Coleman, J. C. Alvarez, S. D. Dreher, R. M. Garbaccio, N. K. Terrett, R. D. Tillyer, M. D. Truppo and E. R. Parmee, *Science, 80,* DOI:10.1126/science.aat0805.

2 T. Bzeih, T. Naret, A. Hachem, N. Jaber, A. Khalaf, J. Bignon, J.-D. Brion, M. Alami and A. Hamze, *Chem. Commun.*, 2016, **52**, 13027–13030.

3 T. Bzeih, K. Zhang, A. Khalaf, A. Hachem, M. Alami and A. Hamze, *J. Org. Chem.*, 2019, **84**, 228–238.

4 B. B. Touré and D. G. Hall, *Chem. Rev.*, 2009, **109**, 4439–4486.

5 J. B. Cox, A. Kimishima and J. L. Wood, *J. Am. Chem. Soc.*, 2019, **141**, 25–28.

6 X. Zhu, C. C. McAtee and C. S. Schindler, *J. Am. Chem. Soc.*, 2019, **141**, 3409–3413.

7 C. He, T. P. Stratton and P. S. Baran, *J. Am. Chem. Soc.*, 2019, **141**, 29–32.

8 R. Barroso, R. A. Valencia, M.-P. Cabal and C. V. Valdés, *Org. Lett.*, 2014, **16**, 2264–2267.

9 C. Johansson Seechurn, C. Carin, M. O. Kitching, T. J. Colacot and V. Snieckus, *Angew. Chem.*, 2012, **51**, 5062–5085.

10 E. Negishi, Ed., *Handbook of Organopalladium Chemistry for Organic Synthesis*, Wiley, New York, 2002.

11 M. Kumada, *Pure Appl. Chem.*, 1980, **52**, 669–679.

12 J. Tsuji, *Palladium Reagents and Catalysts*, Wiley, Chichester, 2004.

13 H. Li, C. C. C. Johansson Seechurn and T. J. Colacot, *ACS Cat.*, 2012, **2**, 1147–1164.

14 C. Ming So and F. Y. Kwong, *Chem. Soc. Rev.*, 2011, **40**, 4963–4972.

15 G. C. Fortman and S. P. Nolan, *Chem. Soc. Rev.*, 2011, **40**, 5151–5169.

16 J. D. Sellars and P. G. Steel, *Chem. Soc. Rev.*, 2011, **40**, 5170–5180.

17 R. Jana, T. P. Pathak and M. S. Sigman, *Chem. Rev.*, 2011, **111**, 1417–1492.

18 A. M. Echavarren, *ChemCatChem*, 2010, **2**, 1331–1332.

19 J. Barluenga, P. Moriel, C. Valdés and F. Aznar, *Angew. Chem.*, 2007, **46**, 5587–5590.

20 Q. Xiao, J. Ma, Y. Yang, Y. Zhang and J. Wang, *Org. Lett.*, 2009, **11**, 4732–4735.

21 J. Barluenga, L. Florentino, F. Aznar and C. Valdés, *Org. Lett.*, 2011, **13**, 510–513.

22 J. Barluenga, M. Tomás-Gamasa, F. Aznar and C. Valdés, *Adv. Synth. Catal.*, 2010, **352**, 3235–3240.

23 J. Barluenga, M. Tomás-Gamasa, P. Moriel, F. Aznar and C. Valdés, *Chem. - A Eur. J.*, 2008, **14**, 4792–4795.

24 Z. Shao and H. Zhang, *Chem. Soc. Rev.*, 2012, **41**, 560–572.

25 J. Aziz, E. Brachet, A. Hamze, J.-F. Peyrat, G. Bernadat, E. Morvan, J. Bignon, J. Wdzieczak-Bakala, D. Desravines, J. Dubois, M. Tueni, A. Yassine, J.-D. Brion and M. Alami, *Org. Biomol. Chem.*, 2013, **11**, 430–442.

26 J. C. Timmerman, N. J. Sims and J. L. Wood, *J. Am. Chem. Soc.*, 2019, **141**, 10082–10090.

27 J. Aziz, J.-D. Brion, M. Alami and A. Hamze, *RSC Adv.*, 2015, **5**, 74391–74398.

28 Q. Zhou, Y. Gao, Y. Xiao, L. Yu, Z. Fu, Z. Li and J. Wang, *Polym. Chem*, 2019, **10**, 569–573.

29 W.-W. Ping, L. Jin, Y. Wu, X.-Y. Xue and X. Zhao, *Tetrahedron*, 2014, **70**, 9373–9380.

30 R. J. Sullivan, G. P. R. Freure and S. G. Newman, *ACS Catal.*, 2019, **9**, 5623–5630.

31 G. T. Thomas, L. MacGillivray, N. L. Dean, R. L. Stoddard, L. P. E. Yunker and J. S. McIndoe, *Int. J. Mass Spectrom.*, 2019, **441**, 14–18.

32 K. L. Vikse, M. P. Woods and J. S. Mcindoe, *Organometallics*, 2010, **29**, 6615.

33 Nanalysis Corp, NMReady-60PRO, https://www.nanalysis.com/nmready-60pro.

34 J. Giberson, J. Scicluna, N. Legge and J. Longstaffe, in *Annual Reports on NMR*

Spectroscopy, ed. G. A. Webb, Elsevier Ltd., London, 2021, vol. 102, pp. 153–246.
35 H. Tan, I. Houpis, R. Liu, Y. Wang, Z. Chen and M. J. Fleming, *Org. Process Res. Dev.*, 2015, **19**, 1044–1048.
36 C. Hansch, A. Leo and R. W. Taft, *Chem. Rev.*, 1991, **91**, 165–195.
37 J. Lu, S. Donnecke, I. Paci and D. Leitch, *ChemRxiv*, DOI:10.33774/CHEMRXIV-2021-QC8VV.
38 D. M. Chisholm and J. Scott McIndoe, *Dalt. Trans.*, 2008, 3933–3945.